

Multiplexing holograms in LiNbO₃:Fe:Mn crystals

Ali Adibi, Karsten Buse, and Demetri Psaltis

California Institute of Technology, Department of Electrical Engineering, Pasadena, California 91125

Received January 19, 1999

Persistent holograms are recorded with red light in lithium niobate crystals doped with manganese and iron. Different erasure mechanisms are investigated, and a recording schedule for multiplexing holograms with equal diffraction efficiencies is proposed. To test the recording schedule experimentally, we multiplex 50 plane-wave holograms with the proposed recording schedule. © 1999 Optical Society of America

OCIS codes: 090.0090, 210.2860, 090.2910.

We recently demonstrated persistent (nondestructive readout) holographic recording in doubly doped lithium niobate (LiNbO₃).¹ Two-center holographic recording is one type of gated holographic recording.^{2–5} In multiplexing many holograms, we need a recording schedule to equalize the diffraction efficiencies of all holograms. There is a well-known recording schedule for the case in which recording and erasure of a single hologram can be represented by monoexponential formulas.⁶ Multiplexing holograms obtained by use of incremental recording have also been investigated for monoexponential recording and erasure dynamics.⁷ In doubly doped crystals, however, the erasure curves are not monoexponential, and therefore a modified recording schedule must be employed. In this Letter we propose and experimentally demonstrate such a recording schedule for multiplexing many persistent holograms in doubly doped LiNbO₃ with equal diffraction efficiencies.

We performed experiments with a congruently melting x-cut LiNbO₃ crystal doped with Fe and Mn. The crystal is oxidized so that initially all Fe traps are empty and a portion of the Mn traps are filled. Illumination with UV light (for example, at 404 nm) excites electrons from Mn centers to the conduction band. A portion of these electrons is trapped by Fe centers. Therefore, the crystal becomes sensitive to red light. Holographic recording is achieved by the simultaneous presence of UV and two red beams interfering in the crystal. The red beams create a charge distribution at the Fe and the Mn trapping sites that is proportional to the interference pattern, and the UV light provides continuous sensitization of the Fe traps. Readout is performed with one red beam only, with no UV light present. During readout, all electrons in the Fe centers will be transferred to the Mn centers. This partially erases the hologram. After all electrons are transferred to the Mn centers, further red readout of the remaining hologram in the Mn traps is nondestructive. A typical recording and readout curve is shown in Fig. 1.

When multiple holograms are recorded, each hologram is erased by both UV and red beams during the recording of subsequent holograms. We performed a series of recording and erasure experiments to assess the dynamics of the processes and to measure the time constants involved. We performed erasure with the

UV light and one of the red beams to get information about the erasure of a hologram while subsequent holograms were recorded. Experimental results for four cycles of recording and erasure are depicted in Fig. 2. The recording curves can be approximated by monoexponential formulas as

$$\sqrt{\eta} = A_0[1 - \exp(-t/\tau_r)]. \quad (1)$$

The erasure curves can be approximated by biexponential formulas as

$$\sqrt{\eta} = A \exp(-t/\tau_{e1}) + B \exp(-t/\tau_{e2}). \quad (2)$$

In Eqs. (1) and (2) η is the intensity diffraction efficiency of the hologram, τ_r is the recording time

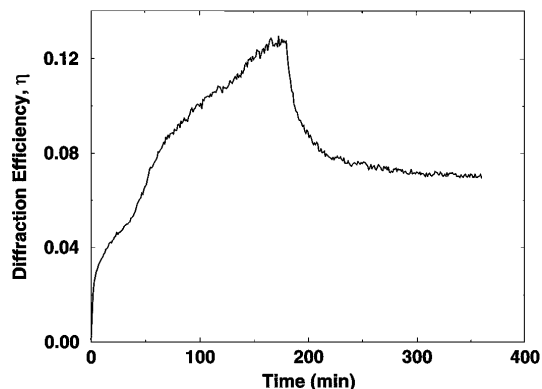


Fig. 1. Recording and readout curve for a plane-wave hologram in a 0.85-mm-thick LiNbO₃ crystal doped with 0.075-wt. % Fe₂O₃ and 0.01-wt. % MnO. The crystal was oxidized for 4 h at 1000 °C in an O₂ atmosphere and then reduced for 1 h at 700 °C in an Ar atmosphere. The UV light is from a 100-W mercury lamp (wavelength, 404 nm, unpolarized; intensity 4 mW/cm², homogeneous), and the two red beams are from a 35-mW He-Ne laser (wavelength, 633 nm, ordinary polarization; 1/e² beam diameter, 2.0 mm; intensity of each beam, 300 mW/cm²). The angle between each beam and the normal to the crystal surface was 21°. The crystal was homogeneously pre-exposed to UV light for at least 1 h before the experiment. Then a plane-wave grating (transmission geometry; grating period, 0.9 μm) was recorded and reconstructed. The grating vector was aligned parallel to the *c* axis of the sample.

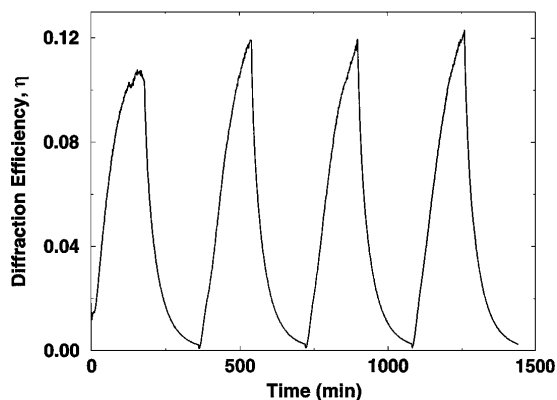


Fig. 2. Diffraction efficiency η versus time for four cycles of recording and erasure with UV and red light in a $\text{LiNbO}_3:\text{Fe}:\text{Mn}$ crystal.

constant, and τ_{e1} and τ_{e2} are the two erasure time constants. Typical mean-square errors in diffraction efficiency for the recording and erasure fits are 2×10^{-8} and 4×10^{-9} , respectively. The biexponential behavior of the erasure is due to the fact that the overall space-charge pattern is the sum of the two space-charge patterns in the Fe and the Mn centers. The space-charge pattern in the Fe centers gets erased (and transferred to the Mn centers) faster than the portion in the Mn centers, owing to the presence of the strong red light. When the whole space-charge pattern settles down in the Mn centers, erasure is performed more slowly, as only UV light can excite electrons from these centers to the conduction band for erasure. Figure 3 shows the effect of different erasure mechanisms. Three different erasure curves after a plane-wave hologram is recorded to saturation are depicted in Fig. 3. These three mechanisms are erasure with UV and one red beam, erasure with UV only, and partial erasure by red light to a steady state and then final erasure by UV only. The curves are normalized so that all three have the same starting point. As Fig. 3 shows, for erasure with red light, only part of the hologram is erased, owing to the transfer of electrons from the Fe to the Mn centers. After all electrons are transferred to the Mn centers, the remaining hologram can be erased with UV light only, and erasure can be represented very well by a monoexponential formula. The hologram can also be erased from the beginning with UV light only, resulting in biexponential erasure.

During hologram multiplexing, each hologram is erased by the UV and the red beams that record the subsequent holograms. Therefore, the erasure is biexponential, and the conventional recording schedule⁶ cannot be used. However, the following observation can lead us to a similar recording schedule: When the holograms are read out at the end of the recording sequence, the electronic charge remaining in the Fe centers is transferred to the Mn centers, resulting in some partial erasure. Erasure during readout is different for different holograms in the sequence. The holograms that are recorded earlier have less charge in the Fe centers than those recorded later in the recording sequence, since the earlier holograms are erased longer than the later ones during the recording sched-

ule. Therefore, the later holograms suffer more from partial erasure during readout. After sufficient readout, this partial erasure is complete for all holograms, and further readout is nondestructive. If each hologram is the sum of a red-erasable part and a non-red-erasable part, we will have only the non-red-erasable part remaining after sufficient readout. During the exposure schedule, this part is erased mainly by UV light (with some help from red light), and its erasure is represented by one of the exponentials (the one with the larger time constant) in Eq. (2). Therefore, we can ignore the red-erasable part, represent the effective erasure with a monoexponential formula, and use the conventional recording schedule⁶ to multiplex many holograms. The $M/\#$ is given by

$$M/\# = \beta A_0 (\tau_{e2}/\tau_r), \quad (3)$$

where β represents the partial loss of the hologram owing to electron transfer from the Fe to the Mn centers. We can measure βA_0 experimentally by recording a grating to saturation and reading it out for a long time with only red light, as shown in Fig. 1. The remaining persistent diffraction efficiency is $(\beta A_0)^2$.

The angular separation of the holograms in angle multiplexing depends on the selectivity of each hologram. Figure 4 shows the angular selectivity curve for one grating. The average angle between the main

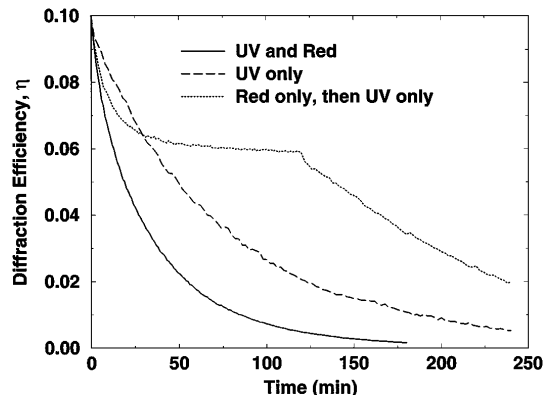


Fig. 3. Normalized diffraction efficiency η versus time for different erasure mechanisms in two-center holographic recording.

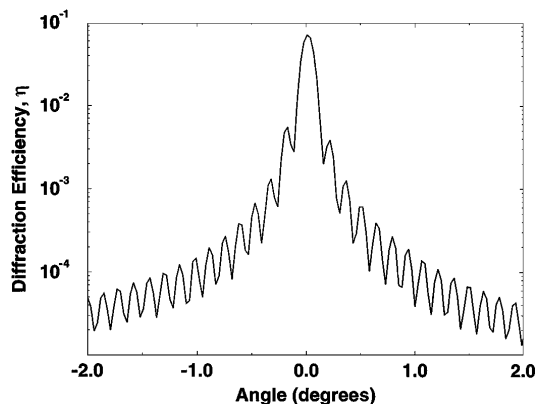


Fig. 4. Selectivity curve for a plane-wave hologram recorded in $\text{LiNbO}_3:\text{Fe}:\text{Mn}$ crystal.

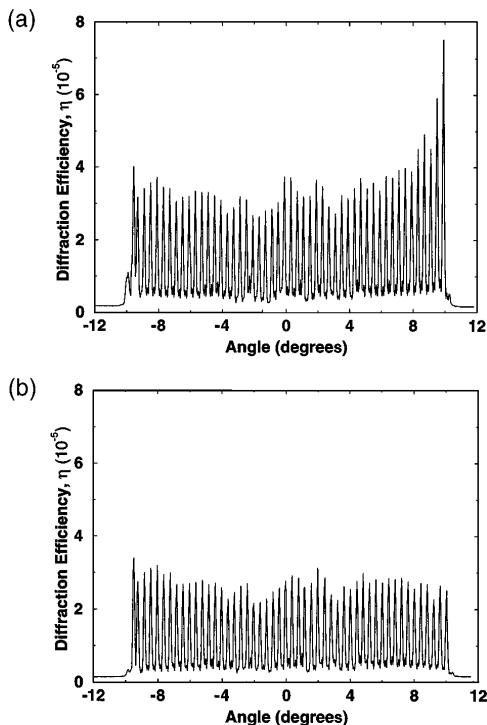


Fig. 5. Diffraction efficiency η versus angle for 50-angle-multiplexed holograms (a) at the end of recording (no readout) and (b) after 1-h readout (exposure by one red beam).

lobe and the first nulls outside the crystal is 0.15° , resulting in an effective thickness of 0.80 mm for the hologram. This effective thickness is smaller than the real thickness of the crystal (0.85 mm), owing to the absorption of the UV beam. Based on Fig. 4, we chose $\theta = 0.4^\circ$ as the angular separation between consecutive holograms.

The recording and erasure time constants for our crystal can be calculated from Fig. 2 as $\tau_r = 4520 \pm 270$ s, $\tau_{e1} = 675 \pm 67$ s, and $\tau_{e2} = 5780 \pm 115$ s. The corresponding recording and readout intensities are given in the caption of Fig. 1. Note that during multiplexing τ_{e1} and τ_{e2} are smaller than the values given above, since erasure is performed by the UV light and both recording red beams. We derived the recording schedule by assuming an effective monoexponential erasure with time constant τ_{e2} . When we multiplex M holograms, the recording time of the n th hologram, t_n , is given by

$$t_n = \frac{\tau_{e2}}{n + R - 1}, \quad (4)$$

where $R = \tau_{e2}/t_1$. In designing the experiment we start with τ_{e2} given above and try to get the best multiplexing performance by fine tuning it. The effect of the partial erasure (given by τ_{e1}) is shown in Fig. 5. Figure 5(a) shows the diffraction efficiency versus angle for 50 plane-wave holograms right after all holograms were recorded, and Fig. 5(b) depicts the same curve after 1 h of readout with red light. Note that partial erasure owing to readout occurs mainly for the last few holograms. We used $\tau_{e2} = 5000$ s and $t_1 = 2500$ s for this experiment. We also measured

$\beta A_0 = \sqrt{0.07} = 0.26$ from Fig. 1. Substituting these values into Eq. (3), we get $M/\# = 0.29$. Based on this $M/\#$, we expect the diffraction efficiency of each hologram to be $\eta = (M/\#/M)^2 = 3.2 \times 10^{-5}$, which is in good agreement with the experimental results.

The incremental recording method can also be used for the doubly doped material, based on the same observation as above, i.e., that each hologram at a specific time is the sum of a red-erasable part (A_e) and a non-red-erasable part (A_{ne}). For multiplexing M holograms, we can represent these portions of each hologram after the $n + 1$ th recording cycle as

$$A_e(n + 1) = \alpha A_0 [1 - \exp(-t_0/\tau_r)] + A_e(n) \exp(-Mt_0/\tau_{e1}), \quad (5)$$

$$A_{ne}(n + 1) = \beta A_0 [1 - \exp(-t_0/\tau_r)] + A_{ne}(n) \exp(-Mt_0/\tau_{e2}), \quad (6)$$

where t_0 and A_0 are the recording time for each hologram in one cycle and the saturation value of $\sqrt{\eta}$, respectively. The erasable and the nonerasable portions of a hologram are represented by α and β , respectively. Since the erasable portion is erased after sufficient readout, we design the incremental recording based on Eq. (6), which is identical to the equation representing incremental recording in a conventional (single-dopant) photorefractive crystal. Therefore, conventional incremental recording⁷ can be employed.

In conclusion, we have demonstrated that the conventional recording schedule can be used for multiplexing holograms with the two-center holographic recording method if the correct erasure time constant is used. Such a recording schedule results in holograms with equal diffraction efficiencies after sufficient readout.

This work was supported by U.S. Air Force/Rome Lab award F0060297C0049 and a Jet Propulsion Laboratory work order funded by Defense Advanced Research Projects Agency/Information Technology Office. K. Buse thanks the Deutsche Forschungsgemeinschaft for a postdoctoral fellowship. D. Psaltis's e-mail address is psaltis@sunoptics.caltech.edu.

References

1. K. Buse, A. Adibi, and D. Psaltis, *Nature (London)* **393**, 665 (1998).
2. D. von der Linde, A. M. Glass, and K. F. Rodgers, *Appl. Phys. Lett.* **25**, 155 (1974).
3. K. Buse, F. Jermann, and E. Krätzig, *Ferroelectrics* **141**, 197 (1993).
4. H. Guenther, G. Wittmann, R. M. Macfarlane, and R. R. Neurgaonkar, *Opt. Lett.* **1305**, 1305 (1997).
5. D. Lande, S. S. Orlov, A. Akella, L. Hesselink, and R. R. Neurgaonkar, *Opt. Lett.* **22**, 1722 (1997).
6. D. Psaltis, D. Brady, and K. Wagner, *Appl. Opt.* **27**, 1752 (1988).
7. Y. Taketomi, J. E. Ford, H. Sasaki, Y. Fainman, and S. H. Lee, *Opt. Lett.* **16**, 1774 (1991).